RNA (1998), *4*:680–693. Cambridge University Press. Printed in the USA.

Localization of hepatitis delta virus RNA in the nucleus of human cells

CELSO CUNHA,[1] JOÃO MONJARDINO,[2] DOROTHY CHANG,[2] SABINE KRAUSE,[3] and MARIA CARMO-FONSECA[1]

[1]Institute of Histology and Embryology, Faculty of Medicine, University of Lisbon, 1699 Lisboa codex, Portugal
[2]Department of Medicine, Imperial College of Science, Technology and Medicine at St. Mary's, London W2, United Kingdom
[3]Department of Cell Biology, Biozentrum, University of Basel, CH-4056 Basel, Switzerland

ABSTRACT

Hepatitis delta virus (HDV) is a human pathogen that can greatly increase the severity of liver damage caused by an hepatitis B infection. HDV contains a circular, single-stranded RNA genome that encodes a unique protein, the delta antigen. Two forms of the delta antigen, δAg-S and δAg-L, are derived from a single open reading frame by RNA editing. Here we analyze the subcellular distribution of HDV RNA and its spatial relationship to known intranuclear structures. The human hepatoma cell line Huh7 was stably transfected with wild-type HDV cDNA and the viral RNAs were localized by in situ hybridization and fluorescence confocal microscopy. HDV RNA is detected throughout the nucleoplasm, with additional concentration in focal structures closely associated with nuclear speckles or clusters of interchromatin granules. Both the smaller form of the delta antigen (δAg-S), which is required for HDV genomic replication, and the larger form of the delta antigen (δAg-L), which represses replication, co-localize with delta RNA throughout the nucleoplasm and in the foci. However, the foci do not incorporate bromo-UTP and do not concentrate either RNA polymerase II or cleavage and polyadenylation factors required for viral RNA synthesis and 3′ end processing, respectively. Thus, it is unlikely that the delta foci represent major sites of viral transcription or replication. In conclusion, the data show that viral RNA–protein complexes accumulate in structures closely associated with interchromatin granules, a subnuclear domain highly enriched in small nuclear ribonucleoproteins, poly(A$^+$) RNA, and RNA splicing protein factors. This implies a specific compartmentalization of ribonucleoproteins in the nucleus.

Keywords: ADAR1; 3′ end processing factors; hepatitis delta virus; interchromatin granules; nuclear organization; RNA localization; splicing factors

INTRODUCTION

Hepatitis delta virus (HDV) was originally discovered as a cause of severe liver disease in patients infected with hepatitis B virus (HBV) (reviewed by Taylor, 1992; Monjardino & Lai, 1993). The clinical association of these two viruses is due to the fact that the outer coat of HDV consists of HBV surface glycoproteins. Thus, productive infection and transmission of HDV requires either co-infection or superinfection with HBV.

The genome of HDV, the smallest animal pathogen known so far, is a single-stranded circular RNA of about 1,700 nt that is ~70% self-complementary and, as a result, forms a highly base paired rodlike structure (see Taylor, 1992). This genomic RNA contains a single open reading frame from which two forms of a unique protein (the delta antigen) are derived by RNA editing. Transcription of the genome results in the synthesis of a 700-nt mRNA that encodes the small form of the delta antigen (δAg-S or HDAg-p24). The larger form of the delta antigen (δAg-L or HDAg-p27) is produced when RNA editing converts an amber stop codon (UAG) to a tryptophan codon (UGG), extending the open reading frame by 19 amino acids (see Taylor, 1992; Monjardino & Lai, 1993). The smaller form of the delta antigen is indispensable for HDV genomic replication (Kuo et al., 1989). In contrast, the larger form represses replication (Chao et al., 1990; Glenn & White, 1991) and is required for packaging of viral particles (Chang et al., 1991; Ryu et al., 1992).

Upon entry into the cell, the genomic HDV ribonucleoprotein complex is transported to the nucleus, where it is replicated by an RNA-directed transcription mechanism that presumably involves cellular RNA polymerase II (MacNaughton et al., 1991; Fu & Taylor, 1993). According to the current model of HDV replication, the incoming HDV genome serves as a template for rolling

Reprint requests to: Maria Carmo-Fonseca, Institute of Histology and Embryology, Faculty of Medicine, University of Lisbon, 1699 Lisboa codex, Portugal; e-mail: hcarmo@fm.ul.pt.

circle replication, resulting in the production of multimeric antigenomes. The nascent antigenomic multimers harbor ribozymes that self-cleave at monomeric intervals. Two self-cleavage events release an antigenomic linear monomer and ligation of its termini produces a circular molecule referred to as the antigenome. Possibly, through a similar rolling circle mechanism, these antigenomes then serve as templates for the subsequent synthesis of genomic RNAs (reviewed by Taylor, 1992; Lazinski & Taylor, 1995).

Editing occurs in the antigenome and is thought to involve a cellular double-stranded RNA-specific adenosine deaminase (dsRAD/DRADA/ADAR1) that converts the adenosine at the amber/W site to an inosine (Casey & Gerin, 1995; Polson et al., 1996; Bass et al., 1997). In addition, maturation of HDV RNAs requires the cellular 3′ end processing apparatus for cleavage and polyadenylation (Hsieh et al., 1990; Hsieh & Taylor, 1991).

Because of its unique features, the study of the HDV life cycle has the potential to unravel novel aspects of RNA metabolism operating in mammalian cells. An important clue to understanding virus–host interactions is the identification of intracellular structures to which the virus is targeted. Although it is generally agreed that both HDV proteins and RNA are predominantly detected in the nucleus, a variety of patterns of intranuclear distribution have been described. In some studies, the delta antigens are localized in the nucleolus, whereas in other reports, they are either in the nucleoplasm or both in the nucleolus and in the nucleoplasm (Taylor et al., 1987; Gowans et al., 1988; MacNaughton et al., 1990a, 1990b; Dourakis et al., 1991; Lai et al., 1991; Negro et al., 1991; Wu et al., 1992; Lazinski & Taylor, 1993; Cullen et al., 1995). In a more recent work, δAg-S was observed in nucleoplasmic speckles associated with those labeled by an antibody directed against the essential splicing factor SC35 (Bichko & Taylor, 1996). However, a precise analysis of the distribution of HDV RNA in the nucleus has not yet been performed. Here, we used fluorescent in situ hybridization combined with immunofluorescence to specifically determine the spatial relationships between HDV RNAs, the small and large forms of the delta antigen, and distinct host cell factors used by the virus.

RESULTS

Intranuclear distribution of HDV RNA

The human hepatoma cell line Huh7 was stably transfected with plasmid pSVL(D3) that contains a trimer of full genomic HDV cDNA cloned in the eukaryotic expression vector pSVL. The cDNA was originally synthesized from total liver RNA derived from an infected woodchuck inoculated with an HDV-containing human serum. The sequence is 1,679 nt long and codes exclusively for δAg-S (Kuo et al., 1988, 1989). Three HDV-expressing clones, D8, D12, and D14, were isolated and expanded as described previously (Cheng et al., 1993). To visualize the integrated HDV genomes, chromosome spreads were prepared from Huh7-D12 cells, denatured and hybridized with plasmid pSVL(D3) labeled with digoxigenin. The hybridization sites were detected using anti-digoxigenin antibody and a secondary antibody conjugated with fluorescein. The hybridization signals, which correspond to transfected HDV cDNAs and are detected in all metaphase spreads, reveal multiple integration sites in a single chromosome (Fig. 1A, arrowhead). In interphase nuclei, the viral cDNAs are detected as clusters of 3–5 fluorescent dots (Fig. 1B, arrow). Con-

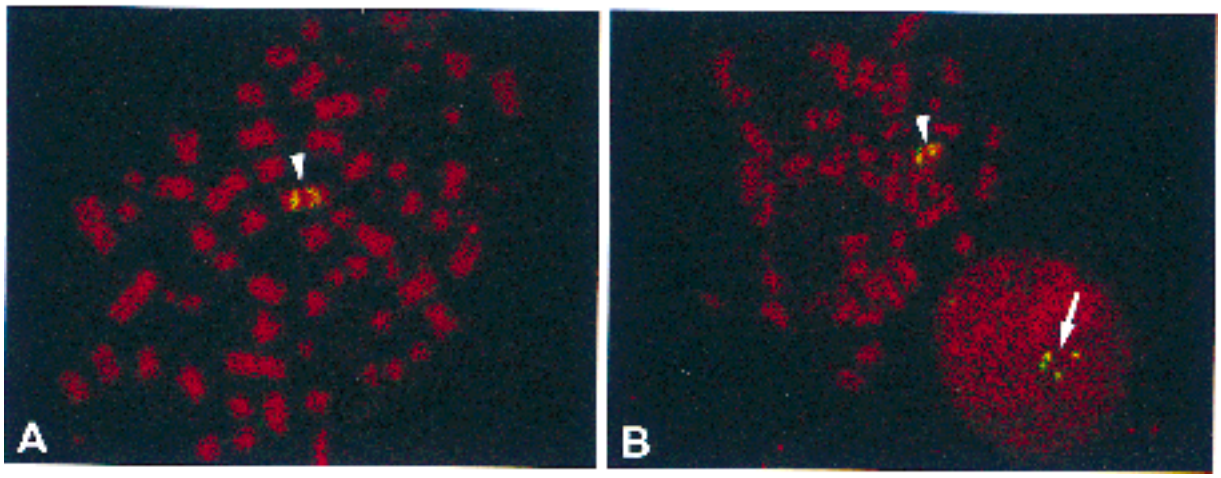

FIGURE 1. Visualization of HDV cDNAs integrated in the genome of Huh7 cells. Metaphase spreads were prepared from Huh7-D12 cells and hybridized with plasmid pSVL(D3), containing the HDV cDNA. Sites of hybridization are detected as green signals. Total DNA is counterstained with propidium iodide (red staining). Arrowheads point to the viral cDNAs integrated in the chromosome. The arrow in B indicates viral cDNAs in an interphase nucleus.

sistent with these observations, clone Huh7-D12 was shown to contain ~40 copies of full-length HDV DNA integrated per haploid genome (Monjardino et al., unpubl. results).

The distribution of HDV RNA was then determined in three-dimensionally preserved Huh7-D12 cells. The pSVL(D3) probe, which hybridizes to both genomic and antigenomic RNA, produces a nucleoplasmic staining pattern, with nucleolar exclusion. In the majority of cells, the nucleoplasmic staining is either finely punctate or coarse-grained with additional 2–20 brighter foci (Fig. 2A,B). In a small number of cells (<10%), the HDV RNA is predominantly scattered throughout the nucleoplasm and does not accumulate in brighter foci. Staining of the nucleolus is never observed. Similar results are obtained when cells are either denatured or nondenatured prior to hybridization. However, the signal intensity is significantly lower and more variable when hybridization is performed under nondenaturing conditions. This probably reflects the highly base paired structure of HDV RNA, and we therefore decided to routinely denature the cells prior to hybridization.

Previous reports have shown that, in vitro, RNA synthesis from both genomic and antigenomic HDV RNA is blocked in the presence of either α-amanitin (1 μg/mL) or a monoclonal antibody specific for RNA polymerase II, suggesting that this cellular enzyme is responsible for the RNA-directed synthesis of viral RNA (MacNaughton et al., 1991; Fu & Taylor, 1993). This prompted us to analyze the distribution of HDV RNA in Huh7-D12 cells treated with α-amanitin. Because exposure of cultured cells to 100 μg/mL α-amanitin for 4 h has been shown to trigger degradation of the largest subunit of RNA polymerase II (Nguyen et al., 1996), Huh7-D12 cells were treated with α-amanitin at concentrations ranging from 100 to 500 μg/mL for 5 h prior

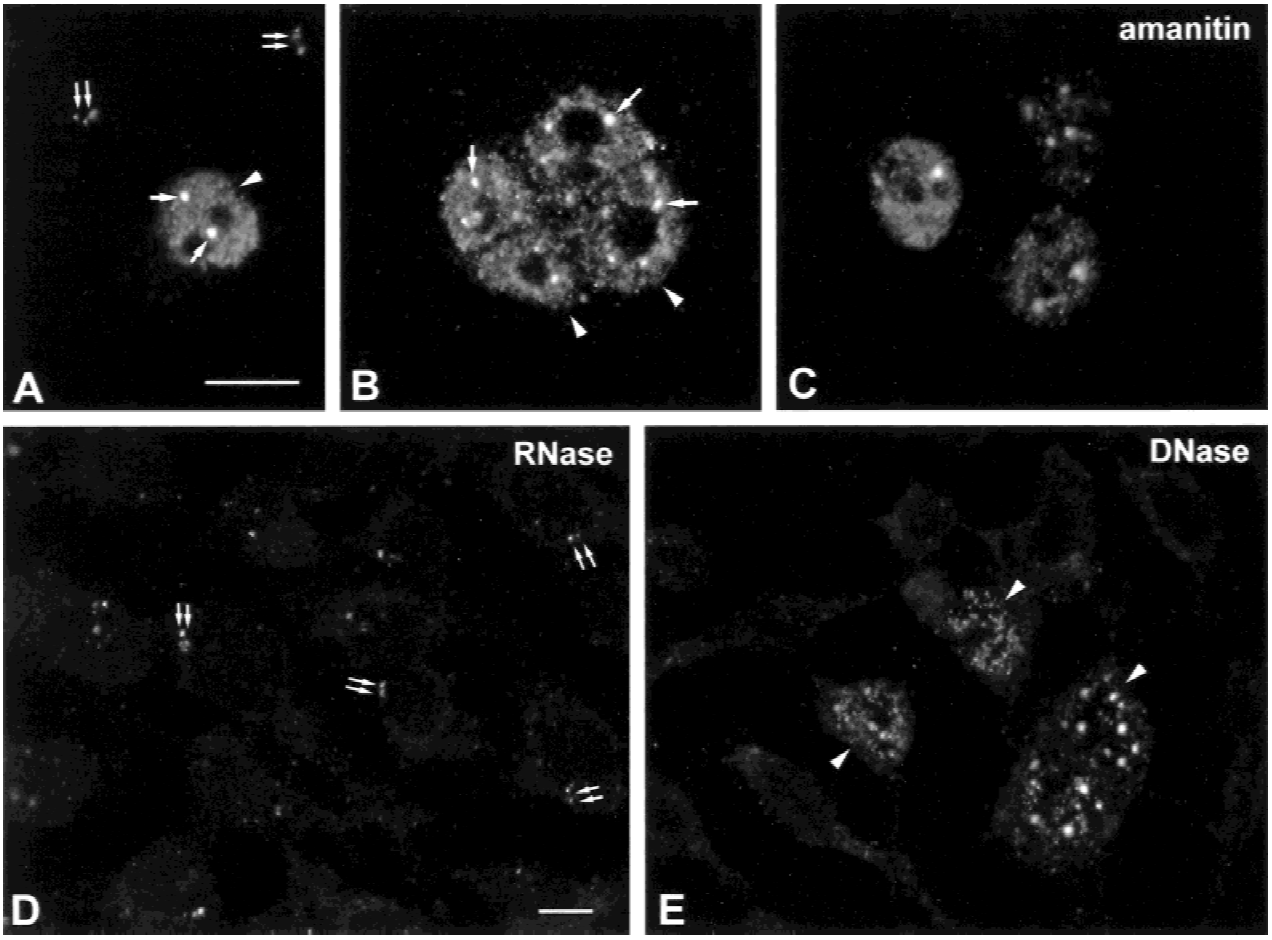

FIGURE 2. Intranuclear distribution of HDV RNA. **A,B:** Huh7-D12 cells were fixed with formaldehyde, permeabilized with Triton X-100, and hybridized with plasmid pSVL(D3). **C:** Cells were treated with 500 μg/mL α-amanitin for 5 h prior to fixation and hybridization. **D:** Cells were treated with RNase A prior to hybridization. **E:** Cells were treated with DNase I prior to hybridization. In A and B (untreated cells), the hybridization signal is either spread throughout the nucleoplasm (arrowheads) or confined to a cluster of fine dots (double arrows); nucleoplasmic staining is finely punctate (A) or coarse-grained (B) with additional brighter foci (A, B, single arrows). The hybridization signal in cells treated with α-amanitin (C) is similar to that of untreated cells. Treatment with RNase abolishes nucleoplasmic staining without affecting the clusters of fine dots (D, double arrows). Inversely, when cells are treated with DNase I, the fine clusters are no longer observed, whereas nucleoplasmic staining with additional concentration in foci is not affected (E, arrowheads). Bar, 10 μm.

to fixation and hybridization. Interestingly, the staining pattern remained similar to that observed in nontreated cells (Fig. 2C), indicating that both the dispersed nucleoplasmic signal and the brighter foci represent stable populations of viral RNAs.

Because cells are denatured before hybridization, the pSVL(D3) probe binds to both the HDV RNA and HDV cDNA integrated in the host chromatin. In order to distinguish between the two, several control experiments were performed. First, nontransfected Huh7 cells were shown not to contain any signal upon denaturation and hybridization. Second, upon treatment of Huh7-D12 cells with RNase A prior to hybridization, complete abolition of the diffuse nucleoplasmic signal and the brighter foci was observed and only the clusters of fine dots were still present in the nucleus of all cells (Fig. 2D, arrows). Finally, treatment of Huh7-D12 cells with DNase I prior to hybridization abolished the clusters of fine dots, but did not affect either the diffuse nucleoplasmic signal or the brighter foci (Fig. 2E). Based on these results, we conclude that the clusters of fine dots present in the nucleus of all Huh7-D12 cells correspond to the transfected HDV cDNA, whereas the scattered nucleoplasmic signal with additional concentration in foci represents HDV RNA. Importantly, these data clearly show that all Huh7-D12 cells contain HDV cDNA, but only a fraction of them is expressing delta RNA.

Co-localization of RNA with δAg-S and δAg-L in nucleoplasmic foci

To compare the distribution of HDV RNA with that of the delta antigens, Huh7-D12 cells were immunolabeled using anti-p24 and anti-p27 antibodies, directed against δAg-S and δAg-L, respectively (Govindarajan et al., 1993). Western blot analysis was performed in order to demonstrate that these antibodies react specifically with the small and large forms of the δAg (Fig. 3A). Furthermore, transient transfection of Huh7 cells with plasmids pSVLAg-S and pSVLAg-L, which encode the small and the large form of δAg, respectively (Chang et al., 1991; Lazinski & Taylor, 1993), confirmed the specificity of each antibody in immunofluorescence experiments (Fig. 3 and data not shown). In transfected Huh7 cells (i.e., in the absence of HDV genomic RNA), δAg-S is predominantly concentrated in nucleoplasmic foci (Fig. 3B,C, arrows), whereas δAg-L is diffuse throughout the nucleoplasm (Fig. 3E,F), and both are present

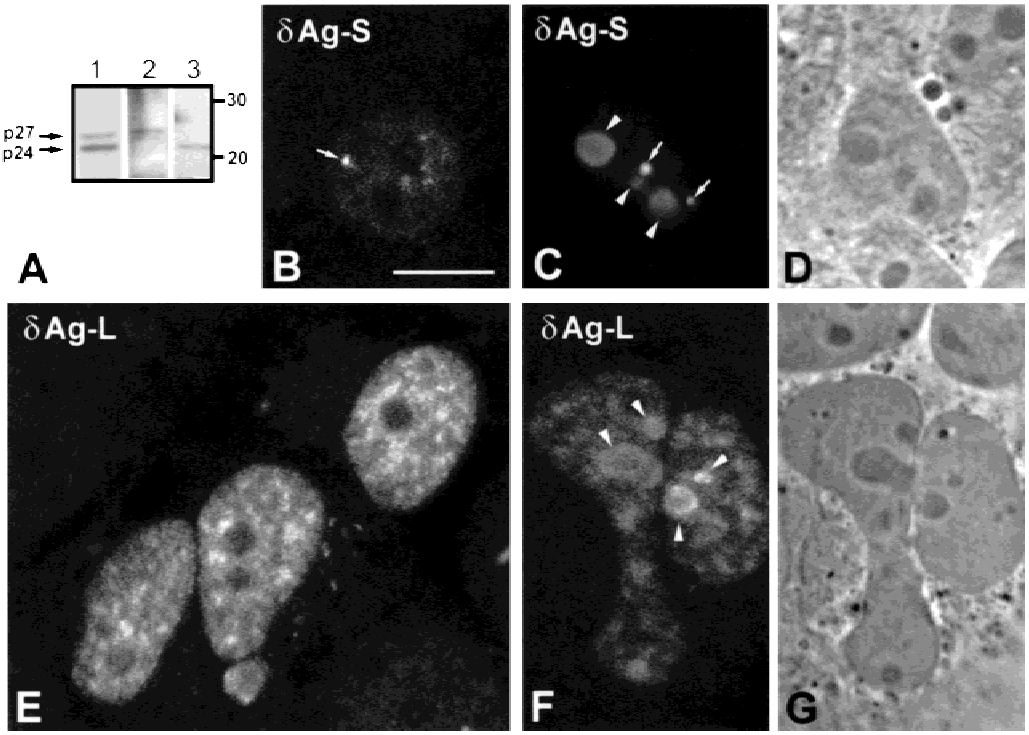

FIGURE 3. Specific identification of the small and large delta antigens. **A:** Total proteins from Huh7-D12 cells were separated in a 10% SDS-polyacrylamide gel, electroblotted onto nitrocellulose filter, and incubated with the B3 antibody (lane 1), polyclonal antibodies specific for the large form of the delta antigen (anti-p27, lane 2), and a monoclonal antibody specific for the small form of the delta antigen (anti-p24, lane 3). Reference molecular mass markers (kDa) are indicated on the right. **B–G:** Intranuclear distribution of delta antigens in cells that do not express viral genomes. Huh7 cells were transfected with either pSVLAg-S (B–D) or pSVLAg-L (E–G), which encode the small and large forms of the delta antigen, respectively (Chang et al., 1991; Lazinski & Taylor, 1993). At 48–72 h posttransfection, the cells were immunostained with either anti-p24 (B–D) or anti-p27 (E–G) antibodies. Arrows point to delta foci and arrowheads point to nucleoli. Panels D and G depict phase-contrast images of the cells shown in E and F, respectively. Bar, 10 μm.

in the nucleolus (Fig. 3C,D,F,G, arrowheads). In contrast to the above observations, in Huh7-D12 cells, the δAg-L is preferentially localized in nuclear foci (>70%), whereas δAg-S is detected in both the nucleoplasm and the foci (>60%). Staining of the nucleolus is only observed in ~10% of the cells labeled with anti-δAg-L antibody (Fig. 4). Taken together, these results are consistent with previous reports indicating that the delta antigens tend to accumulate in the nucleolus in the absence of viral genome replication (Bichko & Taylor, 1996). Additionally, the data show that δAg-S localizes in nucleoplasmic foci even in the absence of HDV genome expression, whereas targeting of δAg-L to the foci depends on expression of the viral genomes.

Finally, double-labeling experiments were performed to compare the localization of δAg-S with that of δAg-L in Huh7-D12 cells, as well as the distribution of HDV RNA with respect to that of delta antigens (Fig. 5). Figure 5A and B and A′ and B′ depict cells double-labeled with an antibody that reacts with both forms of the delta antigen (red staining) and a probe for HDV RNA (green staining). Figure 5C and C′ represents the corresponding superimposition of red and green images. The data show that delta antigens co-localize with delta RNA in nucleoplasmic foci (Fig. 5C, yellow staining); however, delta antigens are detected in nucleoli of cells that do not express delta RNA (Fig. 5C′). Note that the arrows in Figure 5B, B′, C, and C′ indicate HDV cDNA. Figure 5D, E, and F depicts cells double-labeled with antibodies specific for the small (D, red staining) and large (E, green staining) forms of the delta antigen. Superimposition of red and green images confirm that the two forms of the protein are present in the foci (F, yellow staining). In conclusion, the results demonstrate that δAg-S, δAg-L, and δRNA co-localize in the same intranuclear foci.

The delta foci do not correspond to sites of viral RNA synthesis or processing

Previous work from several laboratories has demonstrated that viruses often subvert the host nuclear organization. In particular, adenoviruses have been shown to recruit replication and splicing factors to the sites of active viral replication and transcription (Jiménez-Garcia & Spector, 1993; Pombo et al., 1994). Here we have adapted and extended this approach to investigate the sites of active HDV RNA synthesis and processing in the nucleus of Huh7-D12 cells. Br-UTP was microinjected into the cells, allowed to become incorporated in nascent RNA chains, and detected using an antibody that specifically reacts with brominated nucleotides. The sites of RNA synthesis are visualized as a multitude of fine dots dispersed throughout the nucleoplasm, and no labeling is detected in the delta foci (Fig. 6A,B, arrows). In agreement with this observation, we also do not detect RNA polymerase II in the viral foci (Fig. 6C,D, arrow). Thus, it is unlikely that the foci correspond to sites of active HDV RNA synthesis. This view is also consistent with the finding that the foci contain δAg-L (Fig. 5D,E,F), which is a strong repressor of HDV replication.

In addition to RNA polymerase II, other host cellular factors are thought to be implicated in the HDV life cycle. These include the polyadenylation machinery (Hsieh et al., 1990; Hsieh & Taylor, 1991) and the

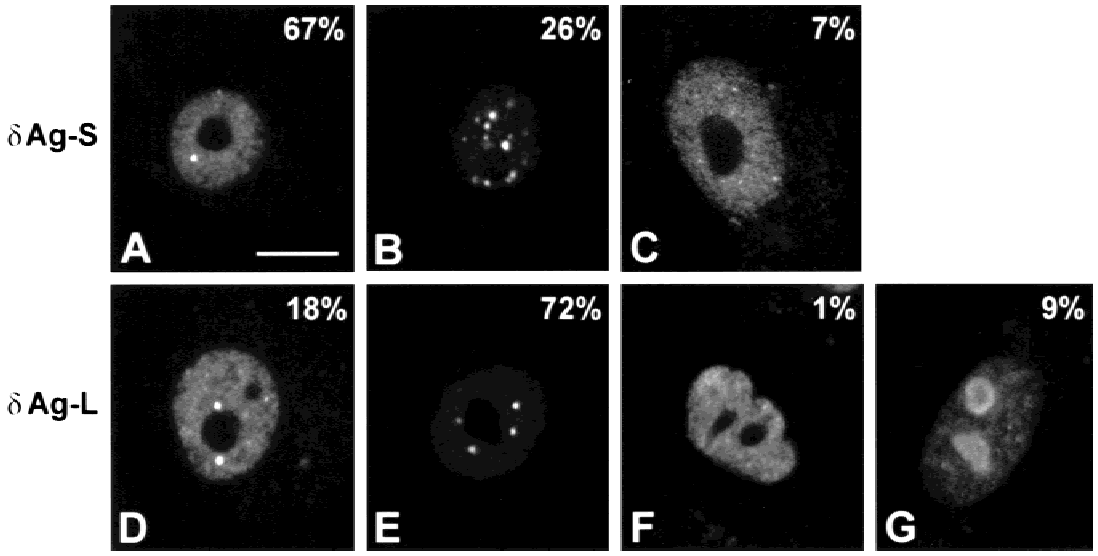

FIGURE 4. Intranuclear distribution of delta antigens in cells that express viral genomes. Huh7-D12 cells were immunolabeled with anti-p24 (**A–C**) or anti-p27 (**D–G**) antibodies. The panel depicts the four distinct labeling patterns observed: (1) diffuse labeling of the nucleoplasm with additional bright foci (A, D); (2) predominant labeling of nucleoplasmic foci (B, E); (3) diffuse labeling of the nucleoplasm with no visible foci (C, F); and (4) labeling of the nucleolus (G). The percentage of each labeling pattern was estimated from a population of approximately 200 cells. Bar, 10 μm.

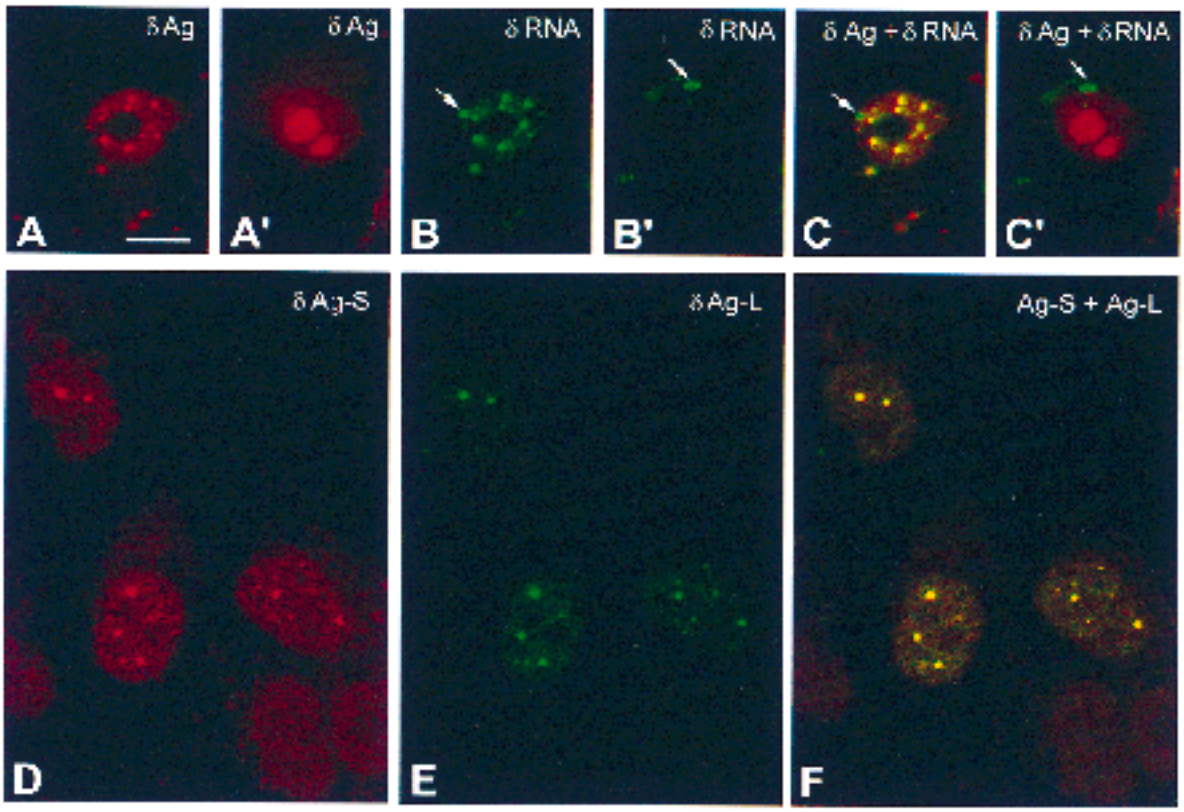

FIGURE 5. Co-localization of HDV RNA and antigens. **A–C, A′–C′:** Huh7-D12 cells were first hybridized with plasmid pSVL(D3) (green staining) and then immunolabeled with B3 antibody (red staining). Panels C and C′ depict a superimposition of panels A and B and A′ and B′, respectively. Panel C shows that both delta RNA and antigens co-localize in the nucleoplasmic foci (yellow staining). Panel C′ shows that cells containing delta antigens in the nucleolus are not expressing delta RNA. Arrows point to HDV cDNA integrated in the cellular genome. **D–F:** Huh7-D12 cells were sequentially labeled with anti-p24 (D) and anti-p27 (E) antibodies. Panel F depicts a superimposition of both images; note that both forms of the delta antigen co-localize in the same foci (yellow staining). Bar, 10 μm.

cellular double-stranded RNA-specific adenosine deaminase (dsRAD/DRADA/ADAR1), which has been implicated in the editing of HDV RNA (Polson et al., 1996). We therefore asked whether HDV induces any major reorganization of components of the polyadenylation machinery or ADAR1 in the nucleus of Huh7-D12 cells expressing δAg.

Because adenovirus requires the host cell cleavage and polyadenylation machinery for the 3′ end processing of its mRNAs, we first studied the effect of this virus on the distribution of poly(A)-polymerase (PAP), cleavage and polyadenylation specificity factor (CPSF), and poly(A) binding protein II (PABII). When adenovirus-infected HeLa cells are probed with antibodies directed against these factors, the nuclear staining pattern changes significantly, depending on the stage of infection. In noninfected cells, PAP and CPSF are distributed diffusely throughout the nucleoplasm with additional concentration of CPSF in "cleavage bodies" (Schul et al., 1996), whereas polyA-binding protein is concentrated predominantly in clusters of interchromatin granules, as described previously (Krause et al., 1994) (data not shown). During the early phase of infection (i.e., before the onset of major viral DNA replication, which occurs at ~8 h postinfection), the staining pattern produced by each antibody is similar to that observed in noninfected cells (data not shown). Following the onset of viral replication (14–18 h postinfection), the normal nuclear architecture is grossly changed and the polyadenylation machinery reorganizes into ring-like structures (Fig. 7A,B,C). Double-labeling experiments confirm that these rings surround the sites of viral DNA, as demonstrated previously for splicing snRNPs and the splicing factor U2AF^{65} (Pombo et al., 1994; Gama-Carvalho et al., 1997).

In Huh7 cells, the distribution of PAP, CPSF, and PAB II is similar to that of noninfected HeLa cells, i.e., PAP and CPSF are distributed diffusely throughout the nucleoplasm with additional concentration of CPSF in cleavage bodies, whereas PAB II is detected predominantly in nuclear speckles. An identical distribution pattern is observed in Huh7-D12 cells and neither of these factors is detected in the viral foci (Fig. 7D,G; E,H; F,I). Thus, in contrast with adenovirus, HDV does not alter the subnuclear distribution of the polyadenylation machinery.

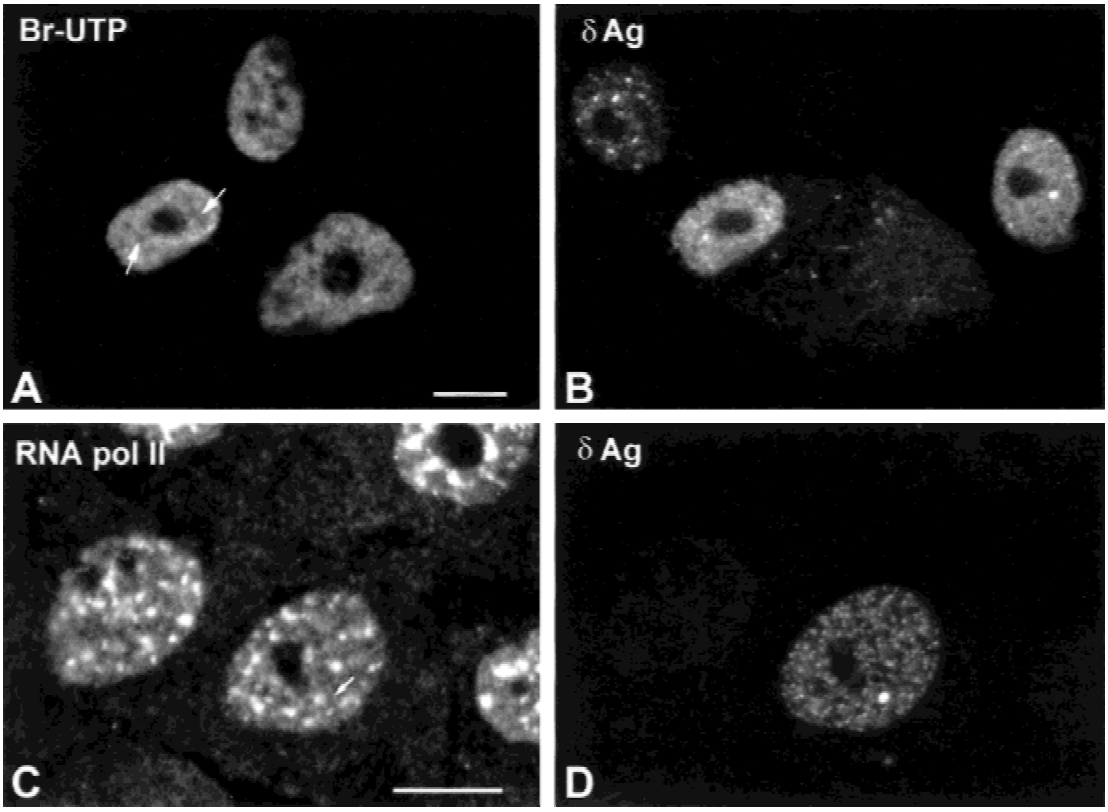

FIGURE 6. The delta foci do not correspond to sites of viral RNA synthesis. **A–B:** Huh7-D12 cells were microinjected with Br-UTP (A) and immunolabeled with B3 antibody (B). **C–D:** Huh7-D12 cells were double-labeled with an antibody directed against RNA polymerase II (C) and B3 antibody (D). Arrows indicate the position of the delta foci. Bar, 10 μm.

In order to analyze the intranuclear distribution of ADAR1, immunofluorescence was performed using rabbit polyclonal antibodies raised and affinity purified against a recombinantly expressed ADAR1 fragment comprising amino acids 167–359 (S. Krause, M.A. O'Connell, & W. Keller, unpubl. data). As depicted in Figure 8, ADAR1 is detected throughout the nucleoplasm of Huh7 cells (Fig. 8A) and, in Huh7-D12, the distribution remains largely unaltered (Fig. 8B,C). Immunofluorescence was also performed using antibodies specific for ADAR2 (O'Connell et al., 1997) and, similarly, no significant redistribution of this enzyme was observed in nuclei expressing HDV (data not shown).

In summary, these data do not support the view that the delta foci represent major sites of HDV RNA synthesis or processing in the nucleus.

The delta foci are closely associated with clusters of interchromatin granules

Finally, we investigated whether the delta foci are randomly localized in the nucleus or associate specifically with known intranuclear structures. At present, it is well established that several nuclear proteins are specifically localized to distinct subnuclear compartments that are detected as dots or speckles by immunofluorescence microscopy (for review, see Spector, 1993). These include coiled bodies, PML nuclear bodies, and clusters of interchromatin granules. Coiled bodies are roughly spherical and vary in size from 0.1 to 1 μm; they consist of coiled $\sim$50-nm threads and contain p80-coilin, some nucleolar proteins, and small ribonucleoprotein complexes involved in pre-mRNA splicing, 3′ end processing of histone transcripts, and rRNA maturation (reviewed by Bohmann et al., 1995). The PML nuclear bodies are spherical or toroidal-shaped, finely fibrillar structures of variable size ($<$1 μm); they contain the PML protein involved in acute promyelocytic leukemia as the consequence of a t(15,17) translocation that generates a PML-RARα fusion capable of disrupting the nuclear body structure (Weis et al., 1994). Interchromatin granules have a diameter of approximately 25 nm and are usually clustered in the interchromatin space, giving rise to irregular-shaped clusters of variable size (Monneron & Bernhard, 1969).

Double-labeling experiments were performed using the B3 antibody that reacts with both forms of the delta proteins (Fig. 9A,B, red staining), and either anti-coilin (Fig. 9A, green staining) or anti-PML (Fig. 9B, green staining) antibodies. As depicted in the figure, some delta foci lie in close vicinity to either coiled bodies or PML nuclear bodies; however, a high proportion ($>$50%)

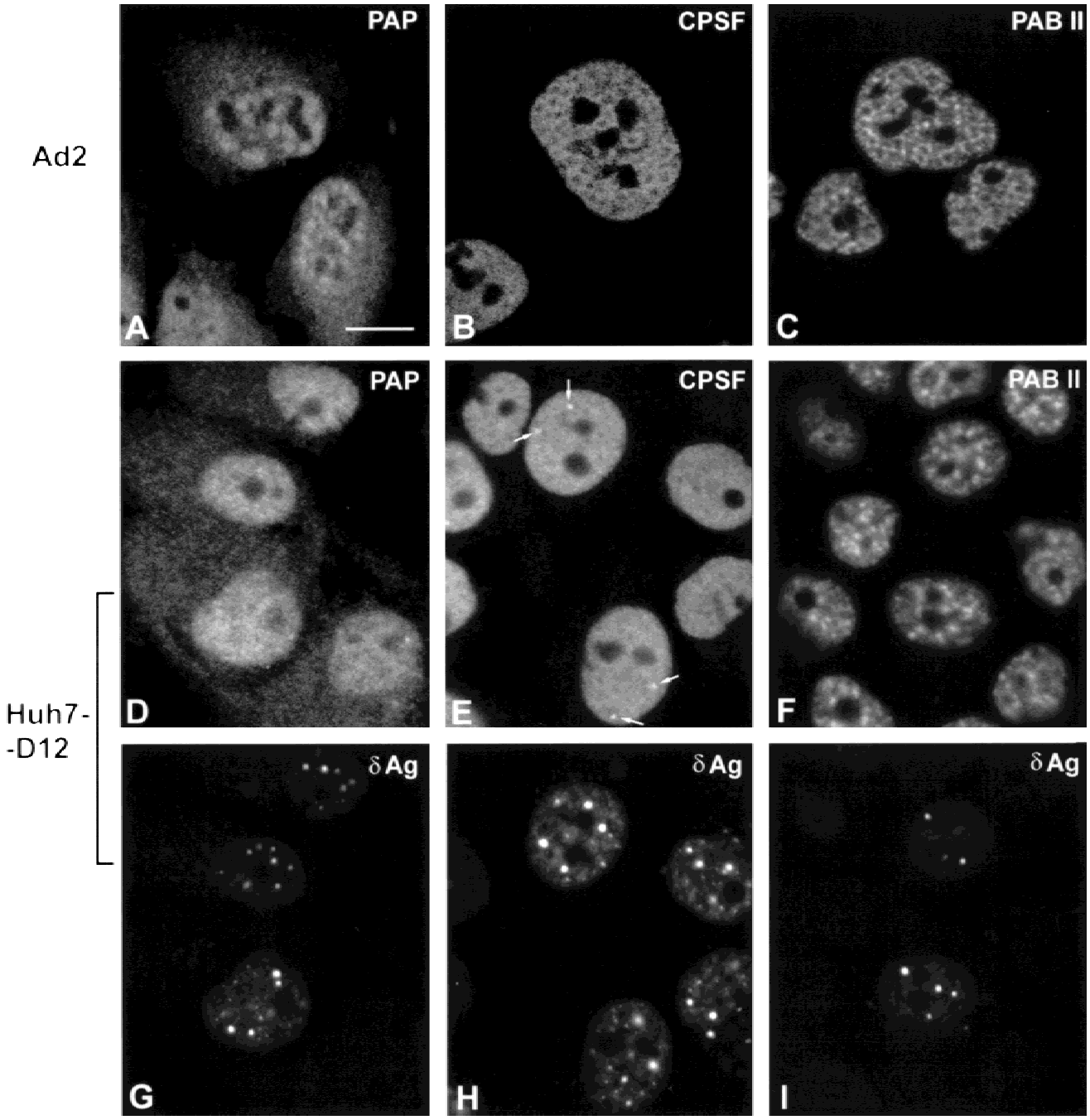

FIGURE 7. Intranuclear distribution of the 3′ end processing machinery. **A–C:** HeLa cells were infected with adenovirus type 2 for 17 h and immunolabeled with antibodies directed against poly(A) polymerase (A), cleavage and polyadenylation factor CPSF-100kDa (B), and poly(A) binding protein II (C). **D–I:** Huh7-D12 cells were double-labeled with anti-PAP, CPSF, or PABII antibodies (D–F) and B3 antibody (G–I). Arrows in E point to "cleavage bodies" (Schul et al., 1996). Bar, 10 μm.

of delta foci appears unrelated to these structures. Considering the high degree of condensation of intranuclear components, this may simply reflect a random distribution of nonchromatin structures within the nucleus.

The spatial distribution of the delta foci was subsequently compared with that of clusters of interchromatin granules. Proteins that are well known to be present in these structures (often referred to as nuclear speckles) in a transcription-dependent manner are the splicing factor SC35 and RNA polymerase II (Spector et al., 1991; Zeng et al., 1997). Double-labeling experiments were performed using the B3 antibody to localize the delta antigens (Fig. 9C,D, red staining) and either SC35 or anti-RNA polymerase II monoclonal antibodies (Fig. 9C,D, green staining). The results clearly indicate that the vast majority of delta foci are in close

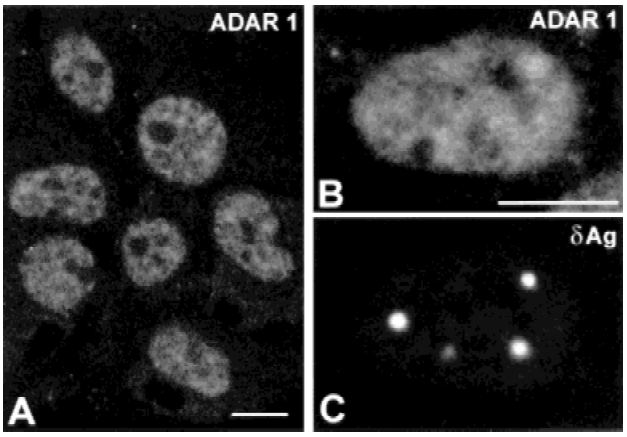

FIGURE 8. Intranuclear distribution of ADAR1 in Huh7 and Huh7-D12 cells. **A:** Huh7 cells labeled with affinity-purified anti-ADAR1 antibodies show a diffuse staining of the nucleoplasm. **B,C:** Huh7-D12 cells were double-labeled with anti-ADAR1 affinity-purified rabbit antibodies (B) and a monoclonal antibody anti-p24 (C). Bar, 10 μm.

proximity but do not co-localize with the clusters of interchromatin granules.

The spatial proximity between HDV foci and clusters of interchromatin granules was further analyzed by immunoelectron microscopy. At this high-resolution level, the delta foci are observed as compact aggregates of electron-dense material adjacent to interchromatin granules (Fig. 10).

DISCUSSION

In the present work, we analyze the subcellular distribution of HDV RNA and its spatial relationship to known intranuclear structures. Althought early studies have localized delta antigens in the nucleolus, more recent data argue against an involvement of this subnuclear compartment in HDV infection because δAg localizes to nucleoli predominantly in the absence of genome replication (Lai et al., 1990; MacNaughton et al., 1990a, 1990b; Bichko & Taylor, 1996). Consistent with this view, we show here that HDV RNA is exclusively localized in the nucleoplasm and that no viral RNA is detected in cells containing antigens confined to the nucleolus. Furthermore, when either the small or the large form of δAg is transiently expressed in Huh7 cells (i.e., cells devoid of HDV genomes), both forms of the protein are frequently localized in the nucleolus. This strongly suggests that the nucleolar accumulation of δAg is caused by protein expression in the absence of appropriate levels of HDV RNA synthesis. In the absence of its target RNA, the delta protein may concentrate in the nucleolus due to its ability to bind RNA nonspecifically at high concentrations and to the high density of RNA present in the nucleolus.

Within the nucleoplasm, HDV RNAs and antigens appear concentrated in discrete spherical nuclear inclusions that we refer to as delta foci. A similar distribution pattern was described previously for δAg-S and proposed to correspond to sites where HDV RNA is transcribed or processed (Bichko & Taylor, 1996). However, the results presented here argue against that interpretation. In fact, the HDV foci do not concentrate either nascent RNA chains, RNA polymerase II, or components of the 3′ end processing machinery. Furthermore, the foci are highly enriched in δAg-L, which represses replication (Chao et al., 1990; Glenn & White, 1991). These results, taken together with the finding that HDV RNAs are dispersed throughout the entire nucleoplasm in addition to being concentrated in the foci, strongly suggest that synthesis and processing of viral RNAs are not confined to discrete sites. This is in agreement with several previous reports demonstrating that RNA biogenesis occurs throughout the nucleus without an obligatory requirement for compartmentalization (reviewed in Fakan, 1994; Carmo-Fonseca et al., 1996; Spector, 1996; Singer & Green, 1997).

If the delta foci are not sites of viral transcription or replication, what may be their role in the nucleus? Based on the data obtained by transient expression of each form of the delta antigen in the absence of viral genome replication, we conclude that δAg-S on its own has the ability to assemble into focal aggregates. Due to its tight interaction with HDV RNA and δAg-L, δAg-S could therefore be responsible for the appearance of the delta foci. Because HDV depends on HBV to supply the envelope proteins required for completion of packaging, secretion, and infection (see Monjardino & Lai, 1993), mammalian cell systems such as Huh7-D12, which are solely transfected with HDV cDNA, fail to export viral particles to the cytoplasm. Thus, the foci may represent depository sites for delta RNA and antigens trapped within the nucleus. In this regard, we are currently analyzing the distribution of HDV components in cells that express HBV envelope proteins.

At present, it is well known that the nucleus contains discrete subdomains that appear as foci or speckles when viewed with the fluorescence microscope. These include different types of nuclear bodies (for review, see Spector, 1993; Bohmann et al., 1995), and we show here that the delta foci are occasionally seen in their close vicinity. However, more than 50% of delta foci are independent from either coiled bodies or PML bodies. In contrast, the delta foci are consistently adjacent to so-called nuclear speckles or clusters of interchromatin granules, which are highly enriched in components of the splicing machinery (Spector, 1993). Although it was initially proposed that nuclear speckles represent preferential splicing sites in the nucleus, subsequent experiments questioned this view. In particular, there are now several lines of evidence indicating that splicing occurs co-transcriptionally and that nascent RNA transcripts are localized at many sites in the nucleus other than clusters of interchromatin granules (reviewed in

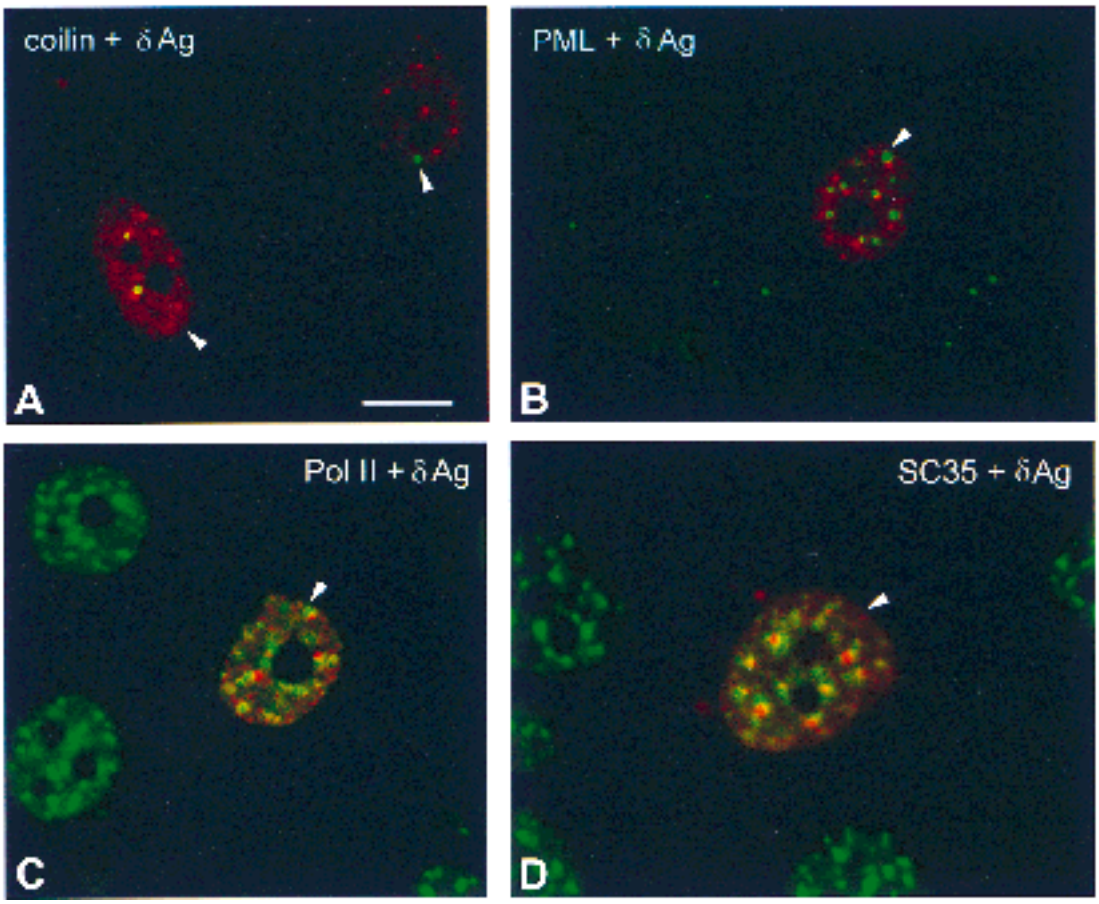

FIGURE 9. Spatial relations of delta foci with host intranuclear structures. Huh7-D12 cells were double-labeled with antibodies directed against p80 coilin (**A**, green staining), PML (**B**, green staining), RNA polymerase II (**C**, green staining), SC35 (**D**, green staining), and B3 antibody (A–D, red staining). Note that, although all Huh7-D12 cells contain HDV cDNA, only a subfraction expresses delta antigens (these are indicated by arrowheads). Bar, 10 μm.

Fakan, 1994; Spector, 1996; Singer & Green, 1997). In addition to splicing factors, RNA polymerase II is also detected in clusters of interchromatin granules (see Zeng et al., 1997 and references therein), and it is now believed that these molecules shuttle between the clusters of interchromatin granules and the sites of active RNA synthesis depending upon transcriptional activity (Misteli et al., 1997). This suggests that the speckles may represent a storage compartment for inactive transcription and splicing factors (Spector, 1993, 1996). Alternatively, it has been proposed that transcription and splicing factors localize to clusters of interchromatin granules for some form of recycling or reactivation between rounds of pre-mRNA synthesis (Bohmann et al., 1995; Zeng et al., 1997).

Experiments using oligo(dT) probes revealed that clusters of interchromatin granules contain polyadenylated RNA (Carter et al., 1991). However, this poly(A)$^+$ RNA is not chased following the inhibition of transcription, arguing that it probably does not represent precursor mRNA in transit to the cytoplasm. Consistent with this view, no individual mRNA species have been detected within the clusters, although several intron-containing genes are transcribed in their periphery (reviewed in Moen et al., 1995; van Driel et al., 1995). In contrast, when cells are infected with either adeno or herpes simplex viruses, the clusters of interchromatin granules enlarge and become highly enriched in viral mRNA (Puvion-Dutilleul et al., 1994; Besse et al., 1995; Bridge et al., 1996), suggesting that these structures may play a role in the intranuclear processing of at least some forms of polyadenylated RNAs (Bridge et al., 1996).

HDV RNAs are shown here to accumulate in foci that are closely associated with clusters of interchromatin granules but, in contrast to the mRNA of DNA viruses, the delta RNA is self-contained within focal structures distinct from the interchromatin granules. Although they are not coincident, the delta foci always appear adjacent to interchromatin granules, suggesting a link between the two structures. One possibility is that the granules somehow attract viral RNA–protein complexes, thereby promoting their assembly. As a consequence, viral ribonucleoproteins become compartmentalized in

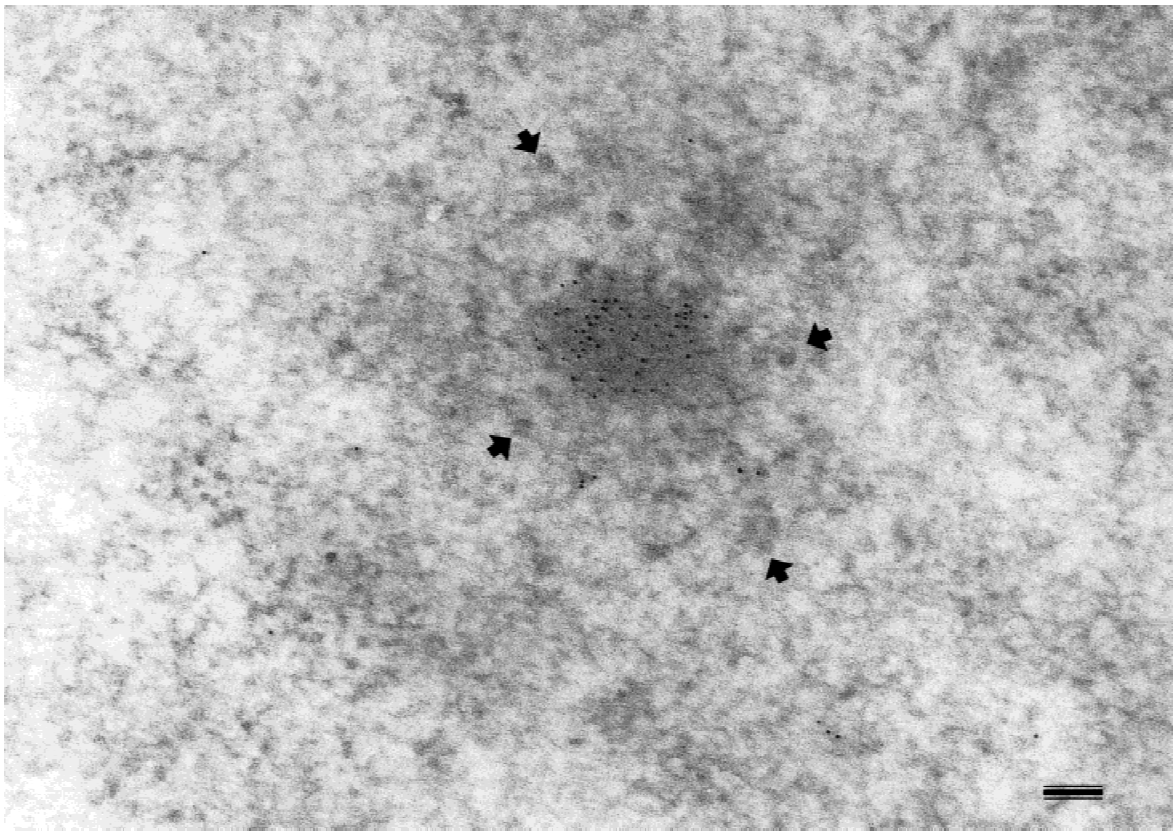

FIGURE 10. Immunoelectron microscopy of delta foci. Thin sections from Huh7-D12 cells were labeled with B3 antibody and antibody-binding sites were revealed with 5-nm colloidal gold particles. Arrows indicate interchromatin granules. Bar, 0.1 μm.

close vicinity to cellular snRNPs and other RNA processing factors.

In summary, the results reported here lead to three main conclusions. First, synthesis of HDV RNA is not confined to specific subnuclear domains, providing further evidence that the nucleus is not compartmentalized with respect to transcription and processing of RNA. Second, the small form of HDV antigen accumulates in focal aggregates in the nucleoplasm, and thereby induces a nonrandom distribution of viral RNA–protein complexes. Third, the focal sites of HDV RNA and protein accumulation are closely associated with clusters of interchromatin granules, suggesting that these structures may act as organizing centers for ribonucleoproteins in the nucleus.

MATERIALS AND METHODS

Cell culture and transfection

Huh7-D12 cells were cultured in Dulbecco's modified minimal essential medium supplemented with 10% fetal calf serum and 200 μg/mL geneticin (G418, Sigma). The cells were grown as monolayers onto 10 $\times$ 10-mm glass coverslips. Transfection of plasmids pSVLAg-S and pSVLAg-L was performed using Lipofectin (Gibco, BRL), according to the manufacturer's instructions. Approximately 2 μg of DNA were used per assay and the cells were analyzed by immunofluorescence at 48–72 h posttransfection.

Fluorescence in situ hybridization

In situ hybridization was performed using pSVL(D3) as a probe. Plasmid pSVL(D3) contains a trimer of full genomic HDV cDNA cloned in pSVL, a eukaryotic expression vector from Pharmacia Biotech. The plasmid was labeled with digoxigenin-11-dUTP (Boehringer Mannheim Biochemicals, Germany) by nick translation (Johnson et al., 1991). In situ hybridization was performed on cytogenetic preparations from Huh7-D12 cells, as described previously (Carvalho et al., 1995). Hybridization in whole cells was performed according to Zirbel et al. (1993). For hybridization under nondenaturing conditions, the cells were treated with 50% formamide at 37 °C for 5 min, whereas for hybridization under denaturing conditions, the incubation was performed in 70% formamide at 75 °C for 5 min followed by an additional 5-min incubation in 50% formamide at 75 °C. For nuclease treatment, the cells were fixed in formaldehyde and permeabilized with Triton X-100 as described below, digested with either DNase I or RNase A, and finally hybridized. For DNase I treatment, the cells were washed twice in 10 mM Tris-HCl, pH 7.5, 25 mM $MgCl_2$, 2 mM DTT, and incubated with 200 U/mL RNase free DNase I (Promega) in the same buffer

containing 50 U/mL RNasin, for 2 h at 37 °C. For RNase A treatment, the cells were washed twice in 10 mM Tris-HCl, pH 7.5, and incubated with 200 μg/mL RNase A (Sigma) in the same buffer for 1 h at 37 °C.

Immunofluorescence and immunoelectron microscopy

For indirect immunofluorescence, the cells on coverslips were rinsed twice in phosphate buffered saline (PBS), fixed with 3.7% formaldehyde (freshly prepared from paraformaldehyde) in PBS for 10 min at room temperature, and subsequently permeabilized with 0.5% Triton X-100 in PBS for 10 min at room temperature. After fixation and permeabilization, the cells were rinsed in PBS containing 0.05% Tween 20 (PBS-T), incubated for 1 h with primary antibodies diluted in PBS-T, washed, and incubated for 1 h with the appropriate secondary antibodies conjugated to either fluorescein or Texas Red (Dianova, Germany; Vector Laboratories, UK). Finally, the coverslips were mounted in VectaShield (Vector Laboratories, UK) and sealed with nail polish.

The following antibodies were used in this study: rabbit polyclonal serum B3 (Saldanha et al., 1990); monoclonal antibody anti-p24, rabbit polyclonal antibodies anti-p27 (Govindarajan et al., 1993); mouse monoclonal antibodies against SC35 (Fu & Maniatis, 1990); RNA polymerase II (CC3; Vincent et al., 1996); p80-coilin (Rebelo et al., 1996); PML (5E10; Weis et al., 1994) and CPSF 100kDa (Jenny et al., 1994); rabbit polyclonal antibodies against PABII (Krause et al., 1994), PAP, ADAR1, and ADAR2 (O'Connell et al., 1997).

Immunoelectron microscopy was performed using a post-embedding method. Huh7-D12 cells were fixed in 3.7% formaldehyde in PBS at 4 °C for 1 h, washed 3 $\times$ 15 min in PBS, dehydrated in an ascending ethanol series, and embedded in Lowycryl. Ultrathin sections were incubated with 0.1 M Tris, pH 7.4, 0.15 M NaCl (Tris-NaCl), 5% BSA, 0.1% gelatin for 15–30 min, incubated with antibody B3 diluted in Tris-NaCl for 1 h at room temperature, washed, and further incubated with a secondary antibody coupled to 5-nm gold particles (Amersham, UK). Sections were then stained with aqueous uranyl acetate.

Visualization of transcription sites

For the detection of nucleoplasmic transcription, 5-bromo-2′-uridine-5′-triphosphate (BrUTP, Sigma, 5mM solution) was microinjected into the cytoplasm of Huh7-D12 cells. The medium was replaced and cells were further incubated for 5–10 min at 37 °C. Cells were then rinsed in PBS and simultaneously fixed and extracted in 3.7% formaldehyde, 0.5% Triton X-100 in HPEM buffer (65 mM PIPES, 30 mM Hepes, pH 6.9, 10 mM EGTA, 2 mM $MgCl_2$) for 15 min at room temperature. The incorporated bromo-uridine was detected using anti-BrdU monoclonal antibody (Boehringer Mannheim) and a secondary antibody labeled with fluorescein. As a control, α-amanitin (0.5 μg/mL) was co-injected with BrUTP (see Carmo-Fonseca et al., 1996). Microinjection was performed using the Eppendorf microinjector 5242. Micropipettes obtained from Clark Electromedical Instruments (Pangbourne, UK) were freshly prepared on a P-87 puller (Sutter Instruments, USA).

Microscopy

Fluorescently labeled samples were analyzed using the laser scanning microscope Zeiss LSM410 equipped with an Argon Ion laser (488 nm) to excite FITC fluorescence and a Helium-Neon laser (543 nm) to excite Texas Red fluorescence. For double-labeling experiments, images from the same focal plane were sequentially recorded in different channels and superimposed. In order to obtain a precise alignment of superimposed images, the equipment was calibrated using multicolor fluorescent beads (Molecular Probes, Eugene, USA), and a dual-band filter that allows simultaneous visualization of red and green fluorescence. Ultrathin sections were examined with a JEOL 100CXII electron microscope operated at 80 kV.

SDS-PAGE and immunoblotting

Cells were washed twice with PBS, mixed with SDS sample buffer, and boiled. Proteins were separated by SDS-PAGE on 10% polyacrylamide minigels (BioRad Laboratories, Richmond, California) and electroblotted to a nitrocellulose membrane at 100 mA for 50 min in 48 mM Tris, 39 mM glycine, 0.04% SDS, 10% methanol. Membranes were blocked and washed in PBS containing 0.1% Tween 20 and 2% low-fat milk powder. Blots were incubated for 1 h with primary antibodies, washed 3 $\times$ 10 min in the same buffer, incubated with the appropriate secondary antibodies conjugated with horseradish peroxidase (BioRad), and developed using a chemiluminescence reaction (ECL, Amersham).

ACKNOWLEDGMENTS

We acknowledge Prof. David-Ferreira for support, Dr. M.A. O'Connell for critical discussions, and Ms. Dora Brito for help with electron microscopy. We are also grateful to the following groups for generously providing materials used in this study: Dr. M. Lai for anti-p27 and p24 antibodies; Dr. Pei-Jer Chen for pSVLAg-S and pSVLAg-L plasmids; Dr. John Taylor for pDL445 plasmid; Dr. Maniatis for SC-35 antibody; Dr. M. Vincent for CC3 antibody; Dr. A. Dejean for anti-PML antibody; and Dr. W. Keller for antibodies against 3′ end processing factors and editing enzymes. This study was supported by grants from Junta Nacional de Investigação Científica e Tecnológica/Program PRAXIS XXI and from the European Union (Human Capital and Mobility Programme). C.C. was supported by a PRAXIS XXI postdoctoral fellowship.

Received January 26, 1998; returned for revision February 2, 1998; revised manuscript received March 23, 1998

REFERENCES

Bass BL, Nishikura K, Keller W, Seeburg PH, Emeson RB, O'Connell MA, Samuel CE, Herbert A. 1997. A standardized nomenclature for adenosine deaminases that act on RNA. *RNA 3*:947–949.

Besse S, Vigneron M, Pichard E, Puvion-Dutilleul F. 1995. Synthesis and maturation of viral transcripts in herpes simplex virus type 1 infected HeLa cells: The role of interchromatin granules. *Gene Expression 4*:143–161.

Bichko VV, Taylor JM. 1996. Redistribution of the delta antigens in cells replicating the genome of hepatitis delta virus. *J Virol 70*:8064–8070.

Bohmann K, Ferreira J, Santama N, Weis K, Lamond AI. 1995. Molecular analysis of the coiled body. *J Cell Sci Suppl 19*:107–113.
Bridge E, Riedel KU, Johansson BM, Pettersson U. 1996. Spliced exons of adenovirus late RNAs colocalize with snRNP in a specific nuclear domain. *J Cell Biol 135*:303–314.
Carmo-Fonseca M, Cunha C, Custódio N, Carvalho C, Jordan P, Ferreira J, Parreira L. 1996. The topography of chromosomes and genes in the nucleus. *Exp Cell Res 229*:247–252.
Carter KC, Taneja KL, Lawrence JB. 1991. Discrete nuclear domains of poly(A)RNA and their relationship to the functional organisation of the nucleus. *J Cell Biol 115*:1191–1202.
Carvalho C, Telhada M, Carmo-Fonseca M, Parreira L. 1995. In situ visualization of immunoglobulin genes in normal and malignant lymphoid cells. *J Clin Pathol Mol Pathol 48*:M158–M164.
Casey JL, Gerin JL. 1995. Hepatitis D virus RNA editing: Specific modification of adenosine in the antigenomic RNA. *J Virol 69*:7593–7600.
Chang FL, Chen PJ, Tu SJ, Wang CJ, Chen DS. 1991. The large form of hepatitis delta antigen is crucial for assembly of hepatitis delta virus. *Proc Natl Acad Sci USA 88*:8490–8494.
Chao M, Hsieh SY, Taylor J. 1990. Role of two forms of hepatitis delta virus antigen: Evidence for a mechanism of self-limiting genome replication. *J Virol 64*:5066–5069.
Cheng D, Yang A, Thomas H, Monjardino J. 1993. Characterization of stable hepatitis delta-expressing cell lines: Effect of HDAg on cell growth. *Prog Clin Biol Res 382*:149–153.
Cullen JM, David C, Wang JG, Becherer P, Lemon SM. 1995. Subcellular distribution of large and small hepatitis delta antigen in hepatocytes of hepatitis delta virus superinfected woodchucks. *Hepatology 22*:1090–1100.
Dourakis S, Karayiannis P, Goldin R, Taylor M, Monjardino J, Thomas HC. 1991. An in situ hybridization, molecular biological and immunohistochemical study of hepatitis delta virus in woodchucks. *Hepatology 14*:534–539.
Fakan S. 1994. Perichromatin fibrils are in situ forms of nascent transcripts. *Trends Cell Biol 4*:86–90.
Fu TB, Taylor J. 1993. The RNAs of hepatitis delta virus are copied by RNA polymerase II in nuclear homogenates. *J Virol 67*:6965–6872.
Fu XD, Maniatis T. 1990. Factor required for mammalian spliceosome assembly is localized to discrete regions in the nucleus. *Nature 343*:437–441.
Gama-Carvalho M, Kraus RD, Chiang L, Valcárcel J, Green MR, Carmo-Fonseca M. 1997. Targeting of $U2AF^{65}$ to sites of active splicing in the nucleus. *J Cell Biol 137*:975–987.
Glenn JS, White JM. 1991. Trans-dominant inhibition of human hepatitis delta virus genome replication. *J Virol 65*:2357–2361.
Govindarajan J, Hwang S, Lai M. 1993. Comparison of the presence of two forms of delta antigen in liver tissue of acute versus chronic delta hepatitis. *Prog Clin Biol 382*:139–143.
Gowans EJ, Baroudy BM, Negro F, Ponzetto A, Purcell RH, Gerin JL. 1988. Evidence for replication of hepatitis delta virus RNA in hepatocyte nuclei after in vivo infection. *Virology 167*:274–278.
Hsieh SY, Chao M, Coates L, Taylor J. 1990. Hepatitis delta virus genome replication: A polyadenylated mRNA for delta antigen. *J Virol 64*:3192–3198.
Hsieh SY, Taylor J. 1991. Regulation of polyadenylation of HDV antigenomic RNA. *J Virol 65*:6438–6446.
Jenny A, Hauri HP, Keller W. 1994. Characterization of cleavage and polyadenylation specificity factor and cloning of its 100-kilodalton subunit. *Mol Cell Biol 14*:8183–8190.
Jiménez-Garcia LF, Spector DL. 1993. In vivo evidence that transcription and splicing are coordinated by a recruiting mechanism. *Cell 73*:47–59.
Johnson CV, Singer RH, Lawrence JB. 1991. Fluorescent detection of nuclear RNA and DNA: Implications for genome organization. *Meth Cell Biol 35*:73–98.
Krause S, Fakan S, Weis K, Wahle E. 1994. Immunodetection of poly(A) binding protein II in the cell nucleus. *Exp Cell Res 214*:75–82.
Kuo MYP, Chao M, Taylor J. 1989. Initiation of replication of the human hepatitis delta virus genome from cloned DNA: Role of delta antigen. *J Virol 63*:1945–1950.
Kuo MYP, Goldberg J, Coates L, Mason W, Gerin J, Taylor J. 1988. Molecular cloning of hepatitis delta virus RNA from an infected woodchuck liver: Sequence, structure and applications. *J Virol 62*:1855–1861.
Lai MMC, Chao YC, Chang MF, Lin JH, Gust I. 1991. Functional studies of hepatitis delta antigen and delta virus RNA. In: Gerin JL, Purcell RH, Rizzetto M, ed. *The hepatitis delta virus. Progress in clinical and biological research*. New York: Wiley-Liss. pp 283–292.
Lai MMC, Lin JH, Xia YP, Chang MF. 1990. Interactions of hepatitis delta antigen with hepatitis delta virus RNA. In: Hollinger FB, Lemon SM, Margolis H, ed. *Viral hepatitis and liver disease*. Baltimore, Maryland: Williams and Wilkins. pp 463–465.
Lazinski DW, Taylor JM. 1993. Relating structure to function in the hepatitis delta virus antigen. *J Virol 67*:2672–2680.
Lazinski DW, Taylor JM. 1995. Regulation of the hepatitis delta virus ribozymes: To cleave or not to cleave? *RNA 1*:225–233.
MacNaughton TB, Gowans EJ, Jilbert AR, Burrell CJ. 1990a. Hepatitis delta virus RNA, protein synthesis and associated toxicity in stably transfected cell lines. *Virology 177*:692–698.
MacNaughton TB, Gowans EJ, McNamara SP, Burrell CJ. 1991. Hepatitis δ antigen is necessary for access of hepatitis δ virus RNA to the cell transcriptional machinery but is not part of the transcriptional complex. *Virol 184*:387–390.
MacNaughton TB, Gowans EJ, Reinboth B, Jilbert AR, Burrell CJ. 1990b. Stable expression of hepatitis delta virus antigen in a eukaryotic cell line. *J Gen Virol 71*:1339–1345.
Misteli T, Caceres JF, Spector DL. 1997. The dynamics of a pre-mRNA splicing factor in living cells. *Nature 387*:523–527.
Moen PT, Smith KP, Lawrence JB. 1995. Compartmentalization of specific pre-mRNA metabolism: An emerging view. *Hum Mol Genet 4*:1779–1789.
Monjardino J, Lai MMC. 1993. Structure and molecular virology. In: Zuckerman, Thomas, ed. *Viral hepatitis*. Churchill Livingstone. pp 329–340.
Monneron A, Bernhard W. 1969. Fine structural organization of the interphase nucleus in some mammalian cells. *J Ultrastruct Res 27*:266–288.
Negro F, Pacchioni D, Bussolati G, Bonino F. 1991. Hepatitis delta virus heterogeneity: A study by immunofluorescence. *J Hepatol 13*:S125–S129.
Nguyen VT, Giannoni F, Dubois MF, Seo SJ, Vigneron M, Kédinger C, Bensaude O. 1996. In vivo degradation of RNA polymerase II largest subunit triggered by α-amanitin. *Nucleic Acids Res 24*:2924–2929.
O'Connell MA, Gerber A, Keller W. 1997. Purification of human double-stranded RNA-specific editase 1 (hRED1) involved in editing of brain glutamate receptor B pre-mRNA. *J Biol Chem 272*:473–478.
Polson AG, Bass B, Casey JL. 1996. RNA editing of hepatitis delta virus antigenome by dsRNA-adenosine deaminase. *Nature 380*:454–456.
Pombo A, Ferreira J, Bridge E, Carmo-Fonseca M. 1994. Adenovirus replication and transcription sites are spatially separated in the nucleus of infected cells. *EMBO J 13*:5075–5085.
Puvion-Dutilleul F, Bachellerie JP, Visa N, Puvion E. 1994. rearrangements of intranuclear structures involved in RNA processing in response to adenovirus infection. *J Cell Sci 107*:1457–1468.
Rebelo L, Almeida F, Ramos C, Bohmann K, Lamond AI, Carmo-Fonseca M. 1996. The dynamics of coiled bodies in the nucleus of adenovirus-infected cells. *Mol Biol Cell 7*:1137–1151.
Ryu WS, Bayer M, Taylor J. 1992. Assembly of hepatitis delta virus particles. *J Virol 66*:2310–2315.
Saldanha J, Homer E, Goldin P, Thomas HC, Monjardino J. 1990. Cloning and expression of an immunodominant region of the hepatitis delta antigen. *J Gen Virol 71*:471–475.
Schul W, Groenhout B, Koberna K, Takagaki Y, Jenny A, Manders EMM, Raska I, van Driel R, de Jong L. 1996. The RNA 3′ cleavage factors CstF64kDa and CPSF100kDa are concentrated in nuclear domains closely associated with coiled bodies and newly synthesized RNA. *EMBO J 15*:2883–2892.
Singer RH, Green MR. 1997. Compartmentalization of eukaryotic gene expression: Causes and effects. *Cell 91*:291–294.
Spector DL. 1993. Macromolecular domains within the cell nucleus. *Annu Rev Cell Biol 9*:265–315.
Spector DL. 1996. Nuclear organization and gene expression. *Exp Cell Res 229*:189–197.

Spector DL, Fu XD, Maniatis T. 1991. Associations between distinct pre-mRNA splicing components and the cell nucleus. *EMBO J 10*:3467–3481.

Taylor JM. 1992. The structure and replication of hepatitis delta virus. *Annu Rev Microbiol 46*:253–276.

Taylor J, Mason W, Summers J, Goldberg J, Aldrich C, Coates L, Gerin J, Gowans E. 1987. Replication of human hepatitis delta virus in primary cultures of woodchuck hepatocytes. *J Virol 61*:2891–2895.

van Driel R, Wansink DG, van Steensel B, Grande MA, Schul W, de Jong L. 1995. Nuclear domains and the nuclear matrix. *Int Rev Cytol 162A*:151–189.

Vincent M, Lauriault P, Dubois MF, Lavoie S, Bensaude O, Chabot B. 1996. The nuclear matrix protein p255 is a highly phosphorylated form of RNA polymerase II largest subunit which associates with spliceosomes. *Nucleic Acids Res 24*:4649–4652.

Weis K, Rambaud S, Lavau C, Jansen J, Carvalho T, Carmo-Fonseca M, Lamond A, Dejean A. 1994. Retinoic acid regulates aberrant nuclear localization of PML-RARα in acute promyelocytic leukemia cells. *Cell 76*:345–356.

Wu JC, Chen CL, Lee SD, Sheen IJ, Ting LP. 1992. Expression and localization of the small and large delta antigens during the replication cycle of hepatitis D virus. *Hepatology 16*:1120–1127.

Zeng C, Kim E, Warren SL, Berget SM. 1997. Dynamic relocation of transcription and splicing factors dependent upon transcriptional activity. *EMBO J 16*:1401–1412.

Zirbel RM, Mathieu UR, Kurz A, Cremer T, Lichter P. 1993. Evidence for a nuclear compartment of transcription and splicing located at chromosome domain boundaries. *Chrom Res 1*:93–106.